Available online at www.sciencedirect.com
ScienceDirect
Advances in Water Resources 31 (2008) 189–202
Advances in Water Resources
www.elsevier.com/locate/advwatres

Calibration of an integrated land surface process and radiobrightness (LSP/R) model during summertime

Jasmeet Judge [a,*], Anthony W. England [b,c], John R. Metcalfe [d], David McNichol [d], Barry E. Goodison [d]

[a] Center for Remote Sensing, Agricultural and Biological Engineering Department, University of Florida, P.O. Box 110570, Gainesville, FL 32611, USA
[b] Department of Electrical Engineering and Computer Science, University of Michigan, 2464 LEC Building, 1221 Beal Avenue, Ann Arbor, MI 48109, USA
[c] Department of Atmospheric, Oceanic, and Space Sciences, University of Michigan, 2464 LEC Building, 1221 Beal Avenue, Ann Arbor, MI 48109, USA
[d] Climate Processes and Earth Observation Division, Climate Research Branch, Meteorological Service of Canada, 4905 Dufferin Street, Downsview, Ontario, Canada M3H 5T4

Received 15 February 2005; received in revised form 31 July 2007; accepted 4 August 2007
Available online 23 August 2007

Abstract

In this study, a soil vegetation and atmosphere transfer (SVAT) model was linked with a microwave emission model to simulate microwave signatures for different terrain during summertime, when the energy and moisture fluxes at the land surface are strong. The integrated model, land surface process/radiobrightness (LSP/R), was forced with weather and initial conditions observed during a field experiment. It simulated the fluxes and brightness temperatures for bare soil and brome grass in the Northern Great Plains. The model estimates of soil temperature and moisture profiles and terrain brightness temperatures were compared with the observed values. Overall, the LSP model provides realistic estimates of soil moisture and temperature profiles to be used with a microwave model. The maximum mean differences and standard deviations between the modeled and the observed temperatures (canopy and soil) were 2.6 K and 6.8 K, respectively; those for the volumetric soil moisture were 0.9% and 1.5%, respectively. Brightness temperatures at 19 GHz matched well with the observations for bare soil, when a rough surface model was incorporated indicating reduced dielectric sensitivity to soil moisture by surface roughness. The brightness temperatures of the brome grass matched well with the observations indicating that a simple emission model was sufficient to simulate accurate brightness temperatures for grass typical of that region and surface roughness was not a significant issue for grass-covered soil at 19 GHz. Such integrated SVAT-microwave models allow for direct assimilation of microwave observations and can also be used to understand sensitivity of microwave signatures to changes in weather forcings and soil conditions for different terrain types.

Keywords: Land surface process model; Microwave remote sensing of soil moisture; Radiobrightness model

1. Introduction

Accurate estimation of water stored in soil, snow, and vegetation that is available to the atmosphere through evapotranspiration, is a functional requirement of the Soil Vegetation Atmosphere Transfer (SVAT) models. These models simulate energy and moisture fluxes at the land surface and in the vadose zone. Examples of some SVAT models include Biosphere Atmosphere Transfer Scheme (BATS) [14,13], Simple Biosphere-2 (SiB-2) model [59], Land Surface Model (LSM) [4], and Variable Infiltration Capacity (VIC) model [41,42]. Typically, SVAT models are linked with Atmospheric General Circulation Models (AGCMs) to predict continental weather and near-term climate. These predictions are highly sensitive to initialization parameters, including the stored water estimates by the SVAT models [2]. Most initialization parameters for the AGCMs, such as atmospheric temperature and moisture

* Corresponding author. Tel.: +1 352 392 1864; fax: +1 352 392 4092.
E-mail address: jasmeet@ufl.edu (J. Judge).

0309-1708/$ - see front matter © 2007 Elsevier Ltd. All rights reserved.
doi:10.1016/j.advwatres.2007.08.006

profiles and sea surface temperatures, are largely derived from satellite observations. Stored water field, however, is initialized with climatic soil moisture due to lack of an operational method for estimating the stored water field from satellites. Recent advances in microwave technology has led to availability of satellites dedicated to providing global soil moisture estimates in the near future [35].

Microwave brightness is sensitive to near-surface soil moisture even through vegetation with green biomass exceeding 5 kg/m^2 – about that of mature corn [28,27,57,24]. This sensitivity of microwaves enables a satellite technique, called four-dimensional data assimilation (4DDA) [54], for improving estimates of near-surface soil moisture. In effect, the technique uses differences between observed and predicted brightness temperatures to correct modeled soil moisture [17,25,21,40,55,54,68,10]. While the brightness is sensitive to moisture only in the upper few centimeters of soil, a microwave emission model can be linked to an appropriate SVAT model to yield soil moisture profiles to depths of a meter or more [6]. The frequently corrected near-surface moisture estimates propagate deeper into the soil to provide improved estimates of the stored water field in the root zone.

To allow direct assimilation of brightness observations, the University of Michigan – Microwave Geophysics Group (UM-MGG) has developed a biophysically based SVAT model that is linked to terrain-specific microwave emission models [45–47,20,36]. Unlike most SVAT models intended for use with atmospheric models, the Land Surface Process (LSP) model is a diagnostic model designed to evaluate our current understanding of the biophysical processes in capturing realistic energy and moisture flow. It simulates one-dimensional coupled heat and moisture transport in unsaturated soils [11,53] when forced with observed downwelling short and longwave radiation, and micro-meteorological observations of air temperature, relative humidity, wind speed, and precipitation. It is initialized with observed soil temperature and moisture profiles. The "base" LSP model has been extended to different terrain and climatic regions. For example, winter wheat in the US Southern Great Plains [33], dry heath in Arctic Tundra [9], and wetland prairie in North Central Florida [70]. It has also been used in climate sensitivity studies [43].

Estimates of soil and canopy moisture and temperatures from these LSP models are used by microwave emission or radiobrightness (R) models to estimate brightness temperatures (see Fig. 1). The estimates of brightness temperatures can then be compared with observed values for data assimilation. The integration of LSP and R models allows for assimilation of observed brightness temperatures directly into the LSP/R model rather than assimilation of empirically derived soil moisture fields (for example, [68,10]).

The objective of this paper is to calibrate a rigorously tested version [30] of the LSP/R model for summertime conditions in Northern Great Plains in the midwestern US. The model is calibrated for bare soil and brome grass using data from our fourth Radiobrightness Energy Balance Experiments (REBEX-4). The calibration was designed to provide best estimates for soil moisture and temperature profiles because brightness signatures are primarily functions of vertical distribution of moisture and temperature in the terrain. In this paper, we briefly describe the observations during REBEX-4, and the LSP/R model. We discuss the calibration methodology and results for bare soil and brome grass. We compare the modeled estimates of temperature and moisture for soil and canopy, and the predicted terrain brightness temperatures at 19 GHz with those observed in the field. Because the LSP model used in this study is a physically based diagnostic model of moisture and energy transport in soil, it provides insights about linkage between control and movement of soil moisture and microwave signature. Integrated LSP/R models can be extended to other, more complex, terrain types to understand the sensitivity of microwave signatures to changes in weather forcings and soil conditions.

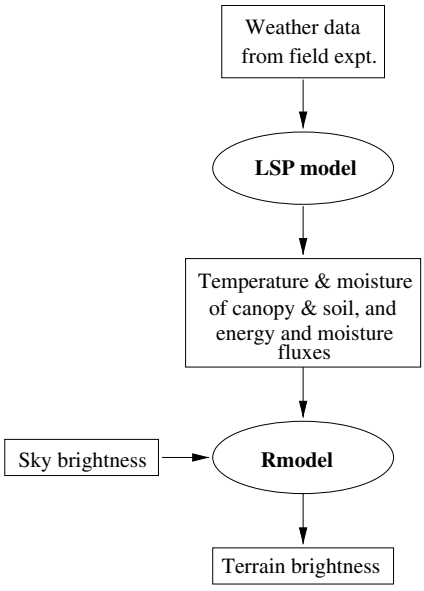

Fig. 1. A flow diagram of interactions between LSP and R model in the LSP/R model.

2. REBEX-4

The REBEXs are series of experiments conducted in relatively homogeneous terrains that are representatives of the selected regions [19,37,32]. These experiments provide unique opportunities to understand microwave signatures of different terrains because ground-based microwave observations are conducted along with measurements of micro-meteorological (henceforth, micromet), soil, and vegetation parameters.

REBEX-4, the experiment that provided the data for this study, was a collaborative experiment conducted jointly with the Climate Research Branch (CRB) of Meteorological Service of Canada, Canada, from June through September in 1996 at the US Geological Survey's Earth

Resources Observation System Data Center, about 30 km north-east of Sioux Falls, South Dakota [31,22,23]. The field site was chosen within 50 m of the REBEX-1 site [19] to obtain a dataset spanning the four seasons for the same location. During the experiment, microwave brightness and micromet parameters were observed for an adjacent artificially created bare soil site and an undisturbed brome grass site concurrently. The bare soil site was prepared by spraying the grass with a herbicide, and ploughing and discing the soil to create a relatively smooth surface. This site was monitored by CRB and the grass site was monitored by the UM-MGG.

Hand-held radiometers at 19.35, 37.0, and 85.5 GHz, developed by the CRB [23], were mounted on a 3 m pole to observe the bare soil site. These radiometers recorded vertical and horizontal polarization measurements every half hour. Switching between the polarizations was carried out using an antenna positioner. The radiometers duplicated the frequencies and the 53.1° incidence angle of the Defense Meteorological Program's Special Sensor Microwave/Imager (SSM/I). A co-located micromet station monitored weather conditions, downwelling and upwelling solar radiation, and net radiation. Brightness temperature and micromet observations were made every 10 min. Soil temperatures and moisture were measured using soil thermistors and Time Domain Reflectometry (TDR) probes, respectively, at depths of 2, 5, and 8 cm at two locations within the site, and soil heat flux was measured at 2 cm-depth at three site locations every 30 min. Soil-core samples were collected for bulk-density measurements twice during the experiment. A detailed description of the bare soil measurements are given in [23,22,29].

UM-MGG observed the grass brightness using a second generation Tower Mounted Radiometer System (TMRS2). It consisted of dual polarized 19.35 and 37.0 GHz, and horizontally polarized 85.5 GHz radiometers atop a 10 m tower. The brightness observations were made every 30 min, while the micromet measurements similar to those at the bare soil site were made every 10 min. Soil temperature was measured at the depths of 2, 4, 8, 16, 32, and 64 cm in two locations at the site every 30 min. Soil heat flux was measured at a depth of 2 cm every half hour at three locations within 2 m of each other. Soil moisture measurements at the grass site were unreliable due to hardware problems with the TDR probes and could not be used for model calibration. Detailed description of the data collected at the grass site is given in [31,29].

3. LSP/R model – biophysics and governing equations

3.1. LSP model

This section briefly describes how the transport of energy and moisture at the land surface and in the vadose zone is simulated by the LSP model. Fig. 2 shows the land surface processes simulated in the model. A detailed description of the model and its numerical validation is provided in [45,29,30].

3.1.1. Vegetation

Vegetation cover is user-defined from 0% (bare soil) to 100% (continuous canopy). The model consists of bi-layered vegetation over a soil. The vegetation includes a photosynthetically active canopy layer and a thermally

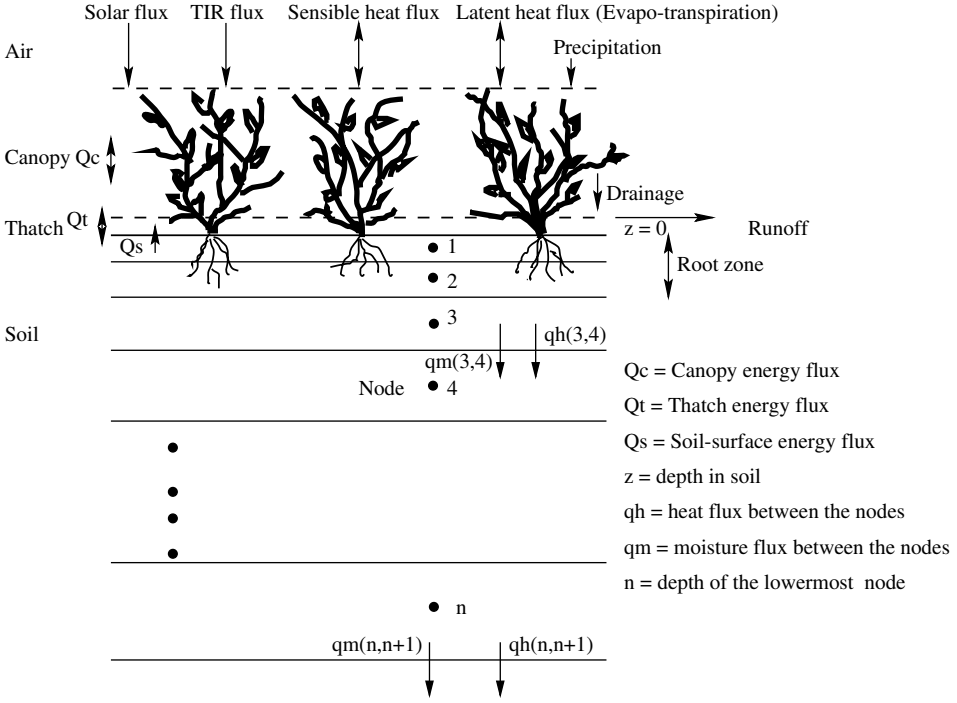

Fig. 2. Land surface processes simulated in the LSP model.

insulating, non-photosynthetic thatch layer. The thatch is very simplistic in the model without moisture holding capacity and does not affect the moisture exchanges between canopy and soil, but it influences the exchange of energy between the soil and the photosynthetically active layer.

The energy fluxes in the vegetation are primarily driven by insolation and TIR emission from the canopy, while moisture fluxes are driven by precipitation and evapotranspiration. The energy and moisture transport equations for the canopy are:

$$\frac{\partial X_{\mathrm{mc}}}{\partial t} = \rho_{\mathrm{l}}(P_{\mathrm{c}} - D_{\mathrm{c}} - E_{\mathrm{tc}}) \quad \frac{\partial X_{\mathrm{hc}}}{\partial t} = -(H_{\mathrm{c}} + L_{\mathrm{c}} - R_{\mathrm{nc}}) \qquad (1)$$

where X_{mc} and X_{hc} are the total moisture and heat contents per unit area stored in the canopy, respectively, (kg/m^2 & J/m^2); ρ_{l} is the density of liquid water (kg/m^3); and P_{c}, D_{c} and E_{tc} are the rates of precipitation, water drainage from the canopy and evapotranspiration (m/s). D_{c} is a function of LAI and E_{tc} is function of aerodynamic resistance and specific humidity, following [67]. H_{c} is the sensible heat flux between the atmosphere and the canopy (W/m^2); L_{c} is the latent heat flux between the atmosphere and the canopy due to evapotranspiration (W/m^2) and; R_{nc} is the net radiation (longwave and shortwave) absorbed by the canopy (W/m^2). The H_{c} is estimated using the bulk transfer approach with aerodynamic resistances given by Trenberth [62], and L_{c} is estimated from H_{c} and Bowen ratio following Peixoto and Oort [52].

3.1.2. Soil

The soil profile with different constitutive properties is divided into 60 computational blocks. Because soil closer to the surface is more influenced by rapid changes in weather and downwelling radiance, thickness of the blocks increase exponentially with depth. The moisture and energy balance equations for the soil are [53,11]:

$$\frac{\partial X_{\mathrm{m}}}{\partial t} = -\nabla \cdot \vec{q}_{\mathrm{m}} \quad \frac{\partial X_{\mathrm{h}}}{\partial t} = -\nabla \cdot \vec{q}_{\mathrm{h}} \qquad (2a)$$

$$X_{\mathrm{m}} = \rho_{\mathrm{l}}(\theta_{\mathrm{l}} + \theta_{\mathrm{v}}) \quad X_{\mathrm{h}} = C_{\mathrm{m}}(T - T_0) + L_0\rho_{\mathrm{l}}\theta_{\mathrm{v}} + \rho_{\mathrm{l}}\int_0^{\theta_{\mathrm{l}}} W\,\mathrm{d}\theta \qquad (2b)$$

$$\vec{q}_{\mathrm{m}} = -\rho_{\mathrm{l}}(D_{\mathrm{T}}\nabla T + D_\theta \nabla\theta + K\hat{k}) \quad \vec{q}_{\mathrm{h}} = -\lambda\nabla T + L_0\vec{q}_{\mathrm{v}} + (c_p q_{\mathrm{v}} + c_{\mathrm{l}} q_{\mathrm{l}})(T - T_0) \qquad (2c)$$

where X_{m} is the total moisture content per unit volume (kg/m^3); $\vec{q}_{\mathrm{l}}$, $\vec{q}_{\mathrm{v}}$, and $\vec{q}_{\mathrm{m}}$ are the liquid, vapor and moisture flux densities (kg/m^2 s), respectively; ρ_{l} is the density of liquid water (kg/m^3); θ_{l} and θ_{v} are the volumetric liquid water (m^3/m^3) and vapor content (m^3 of precipitable water/m^3), respectively; $\theta = \theta_{\mathrm{l}} + \theta_{\mathrm{v}}$; T is the absolute temperature (K); D_{T} and D_θ are the thermal and isothermal moisture (liquid and vapor) diffusivities (m^2/K s), respectively; K is the unsaturated hydraulic conductivity (m/s); X_{h} is the total heat content per unit volume (J/m^3); $\vec{q}_{\mathrm{h}}$ is the heat flux density (J/m^2 s), respectively; C_{m} is the volumetric heat capacity of moist soils (J/m^3 K); c_p and c_{l} are the specific heats (J/kg K) of water vapor at constant pressure and of liquid water, respectively; L_0 is the latent heat of vaporization (J/kg) at the reference temperature, T_0; W is the differential heat of wetting; and λ is the thermal conductivity of soil (J/m K s).

The constitutive properties of soil, such as moisture and thermal diffusivities, tortuosity, thermal conductivity, and water retention, are estimated from empirical models that have earned acceptance in the literature [11,12,38,39,56,45]. When vegetation is present, the upper blocks also serve as a root-zone where moisture for transpiration is drawn from the soil, as shown in Fig. 2. The suction from root zone affecting the latent heat flux is modeled following Verseghy et al. [67] and Noilhan and Planton [51].

The moisture and energy fluxes across the upper boundary, i.e., at the interface between soil and vegetation, are driven by net precipitation and radiation reaching the soil surface as follows:

$$q_{\mathrm{m}}(0,1) = \rho_{\mathrm{l}}(D_{\mathrm{c}} - E_{\mathrm{s}} - E_{\mathrm{tr}} - \mathrm{Runoff})$$
$$q_{\mathrm{h}}(0,1) = R_{\mathrm{ns}} - H_{\mathrm{s}} - L_{\mathrm{s}} \qquad (3)$$

where $q_{\mathrm{m}}(0,1)$ and $q_{\mathrm{h}}(0,1)$ are the moisture and heat flux densities at the interface between blocks 0 (vegetation) and 1 (soil surface), respectively; H_{s} and L_{s} are the sensible and latent heat fluxes from the soil, respectively (W/m^2); D_{c} is the rate of drainage from the canopy (m/s); D_{c} = total precipitation − interception by the canopy; E_{s} is the rate of evaporation from the soil (m/s); E_{tr} is rate at which water is extracted from the root zone to maintain transpiration (m/s); and R_{ns} is the net radiation (longwave and shortwave) absorbed by the soil (W/m^2). The H_{s} and L_{s} are estimated using bulk transfer approach and Bowen ratio similar to that used for the vegetation.

The energy and moisture fluxes across the lower boundary, i.e., at the interface between the nth and $n+1$th computational blocks, are set equal to the fluxes across the interface between $n-1$th and nth block (see Fig. 2). This allows no change in the moisture and heat content of the nth block.

The non-linear and coupled equations for conservation of moisture and energy in soil (Eq. (2a)) are linearized and solved using an explicit, forward finite difference method [6,47]. It uses a block-centered grid where the soil parameter values for each computational block are assumed to be located at the center of that block. In the model, the dynamic response to non-linearity is lagged in time. Fig. 3 gives a flow diagram of how the transport processes are simulated in the LSP model. To begin, the soil and the vegetation properties are initialized and the initial energy and moisture fluxes are calculated. The model is forced with weather, and a two-dimensional Newton–Raphson technique is applied in conjunction with a finite difference method to balance energy and moisture fluxes at the soil surface. The boundary-flux matching process is

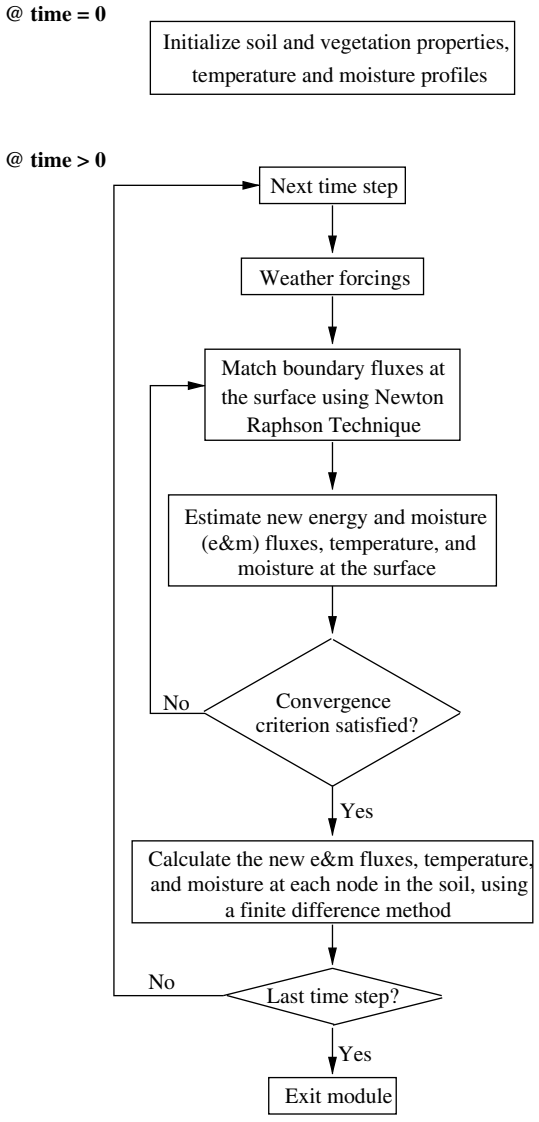

Fig. 3. A flow diagram of the LSP model algorithm.

repeated until a specified convergence criterion is satisfied. The resulting new fluxes are used to estimate the new surface temperature and moisture. Once the surface temperature and moisture are estimated, the difference method is employed to calculate the new fluxes, temperature, and moisture for each soil block [30].

3.2. R model

The R model estimates the non-scattering emission from a canopy layer modeled as an isothermal, homogeneous dielectric layer (canopy-cloud), over a semi-infinite, homogeneous, and smooth-surfaced soil. The brightness of the terrain, T_b, is:

$$T_b = T_{bs} + T_{bc,d} + T_{bc,u} + T_{bsky} \quad (4)$$

where T_{bs} is the emission from soil at the top of the canopy after being attenuated through the canopy (K); $T_{bc,d}$ is the downwelling emission from the canopy reflected by the soil and attenuated through the canopy (K); $T_{bc,u}$ is the upwelling emission from the canopy (K); and T_{bsky} is the downwelling sky emission reflected by the soil and attenuated through the canopy (K).

The emission from soil depends upon the effective temperature and reflectivity of the soil. The effective temperature is estimated as a first order approximation using temperature gradient between the first two nodes of the soil in the LSP model (top 2 cm). The relative permittivity and reflectivity of the soil are estimated from a four-component mixture model by Dobson et al. [15] and Fresnel equations, respectively. The emission from the canopy depends upon the temperature (isothermal in our case) and the relative permittivity of the canopy. The relative permittivity is estimated from the dual-dispersion model by Ulaby and El-Rayes [63]. The attenuation through the canopy depends on its optical depth (τ), which is modeled empirically following [16,66], and is given by:

$$\tau = -\frac{2kn_cB_c}{\rho_c} \quad (5)$$

where ρ_c is the density of wet vegetated material (kg/m^3); n_c is the complex refractive index of the canopy; B_c is the wet biomass of the canopy (kg/m^2); and k is the wave number.

4. LSP/R model simulation for REBEX-4

4.1. Input variables

The LSP component of the integrated model was forced with downwelling solar radiation, wind speed, air temperature, relative humidity, and precipitation observed during REBEX-4. The downwelling longwave radiation was not measured during REBEX-4, and was estimated from the observed downwelling and upwelling solar radiation, net incoming radiation, and soil TIR temperature.

The R component of the model was forced with estimates of temperature gradients in the top two nodes, moisture and temperatures of the soil surface and the canopy from the LSP model. Vegetation density and biomass were obtained from REBEX-4. The sky brightness observed during REBEX-4 could not be used because of calibration problems at colder temperatures [36]. From our earlier studies, the sky brightness at 19 GHz were found to vary between 20 and 60 K, as estimated from the expressions given by Ulaby et al. [64] using temperature and density profiles from rawinsonde data at Huron, South Dakota, about 200 km from the REBEX-4 site [18,34]. The sky brightness were assumed to be 20 K for clear and 50 K for cloudy days for the calibration.

4.2. Initial conditions

REBEX-4 observations provided the initial conditions for moisture and temperatures for canopy, thatch, and soil (upper 8 cm at the bare soil site). The initial soil moisture values for the upper 24 cm at the grass site were obtained

from a diurnal experiment conducted three days before beginning of the calibration period. During this experiment, three gravimetric measurements were made of soil moisture in the top 24 cm using every 2 h for 24 h, using a coring tool. The temperature profiles for the deeper layers for both the sites were estimated from an annual model [44]. The soil moisture profiles was linearly interpolated for the soil nodes between 8 cm. The water table was located at 2 m [3] near the bare-soil site, and between 24 cm and 2 m for the grass site. Deeper than 2 m, the soil was saturated and the moisture content was equal to porosity.

4.3. Soil properties

The soil at the REBEX-4 site was a silty clay loam. Estimates of soil texture, wilting point, and field capacity were obtained from a soil survey report [50]. However, at the grass site, there was organic matter in the upper 5 cm of the soil. Estimated range of porosities, 46–50%, were obtained from the bulk density calculations during REBEX-4. The roughness length of the soil, i.e., the height above the surface where the wind speed vanishes, was estimated from [60]. The physical properties used by the LSP/R model for the upper 5 cm are tabulated in Table 1.

Thermal conductivity, as a function of soil constituents, particle shape, and moisture, was from an empirical model by de Vries [12]. For simplicity, the shape of the soil particles were assumed to be spherical. During the model simulation, the thermal conductivity of soil varied between 0.58 and 0.65 W/m K.

Soil hydraulic conductivity is modeled based upon two parameter junction model [56,49]. The saturated conductivity was the only unconstrained constitutive property in the bare soil model, and its value for each node was varied within the allowed range Nestrud et al. [50], Judge and England [31] to calibrate the model. The assigned values that provided the best calibration results were 2×10^{-7} m/s in the top 1 cm of soil and 5×10^{-7} m/s in the next 4 cm.

Two parameters in the model describe the radiation properties of the soil, viz., TIR emissivity and shortwave albedo. The emissivity for bare bare soil was set to 0.96 in the model [52]. The albedos of most agricultural soils vary between 0.2 and 0.4 [1], but are functions of solar angle, cloud cover, soil physical properties such as color and roughness [60], and soil moisture [26]. For the bare soil site, we used a variable albedo obtained by fitting observed values to cubic polynomials for clear and cloudy days as functions of the solar angle. For the grass site, the soil albedo was a constant at 0.33.

For the R model, the dielectric constant for the dry soil solids was 4.0 [65]. The soil was specular, incoherent, multilayer emitter with dielectric permittivity from four-component mixing model developed by Dobson et al. [15].

4.4. Vegetation properties

During the calibration period, the brome grass canopy was fully mature with an average height of 70 cm. In general, the leaf area index (LAI) for mature grass canopies ranges between 2 and 4 [47]. We found that LAI = 3.5 provided the best fit between the model estimates and the observations. Because the REBEX-4 grass site had been undisturbed for several years, the thatch was approximately 2–3 cm thick and accounted for ~25–30% of the canopy weight [29]. It was modeled as dead vegetation with a transmissivity and heat capacity the same as dry vegetation. Table 2 gives the canopy properties included in the model. The albedo of the canopy was estimated by curve-fitting the observed values for a clear and a cloudy day, following the same procedure as for the bare soil. For the R model, the dielectric properties of the canopy were estimated from a dual-dispersion model by Ulaby and El- Rayes [63].

4.5. Solution convergence

Because the R model is numerically simplistic, only the LSP model was tested for solution convergence before calibration. The model was run using different spatial (node spacing) and temporal (time steps) resolutions [29]. The soil temperature and moisture estimates converged i.e., the model estimates of moisture and temperature profiles did not change as the time interval between each model update, or the time steps, decreased. Similar convergence was achieved as the inter-nodal distances decreased. In general, the time steps and inter-nodal distances at which the solution converges depend upon the soil properties and the strength of forcings at the upper boundary. The soil was

Table 1
Soil physical properties in the upper 5 cm at the REBEX-4 sites

Properties	Bare Soil Site	Grass Site	
	0–5 cm	0–1 cm	0–5 cm
Silt fraction (%)	65.1	60	25
Clay fraction (%)	31.0	30	2.5
Sand fraction (%)	3.9	1	1
Organic fraction (%)	0.0	8	71.5
Field capacity (m^3/m^3)	0.294	0.294	0.294
Wilting point (m^3/m^3)	0.145	0.145	0.145
Porosity (%)	48.0	50	50
Roughness length (m)	0.02–0.09	0.02–0.09	0.02–0.09

Table 2
Canopy properties at the REBEX-4 grass site

Properties	Values
LAI	3.5 [unconstrained parameter]
Root depth (cm)	25 [31]
Height (hc) (cm)	70 [31]
IR emissivity	0.95 [62]
Roughness length	0.2 × hc [67]
Displacement height	0.65 × hc [67]

discretized into 60 nodes with eight nodes in the top 5 cm during the simulation. For a 5-day simulation, the model estimated profiles achieved convergence when the time-step was decreased to 3 s. A further decrease in the time-step to 2 or 1.5 s produced changes in the moisture and temperature estimates of $\leqslant 0.04\%$ by volume and $\leqslant 0.05$ K, respectively.

As the number of nodes in the top 5 cm increased from 3 to 8, the temperature and water column estimates oscillated within ~ 0.05 K and 0.2 mm/m^2, respectively. The oscillations decreased by half, as the number of nodes increased from 8 to 13. For all the model simulations presented in this paper, the time step was 3 s and the soil was discretized into 60 nodes with eight nodes in the upper 5 cm.

4.6. Results and discussion

4.6.1. Bare soil

The bare soil conditions were simulated for 25 days, from Day of Year (DoY) 193 (July 12) through 218 (August 5) in 1996. Fig. 4a–d show comparisons of model estimated and REBEX-4 measured soil temperatures at

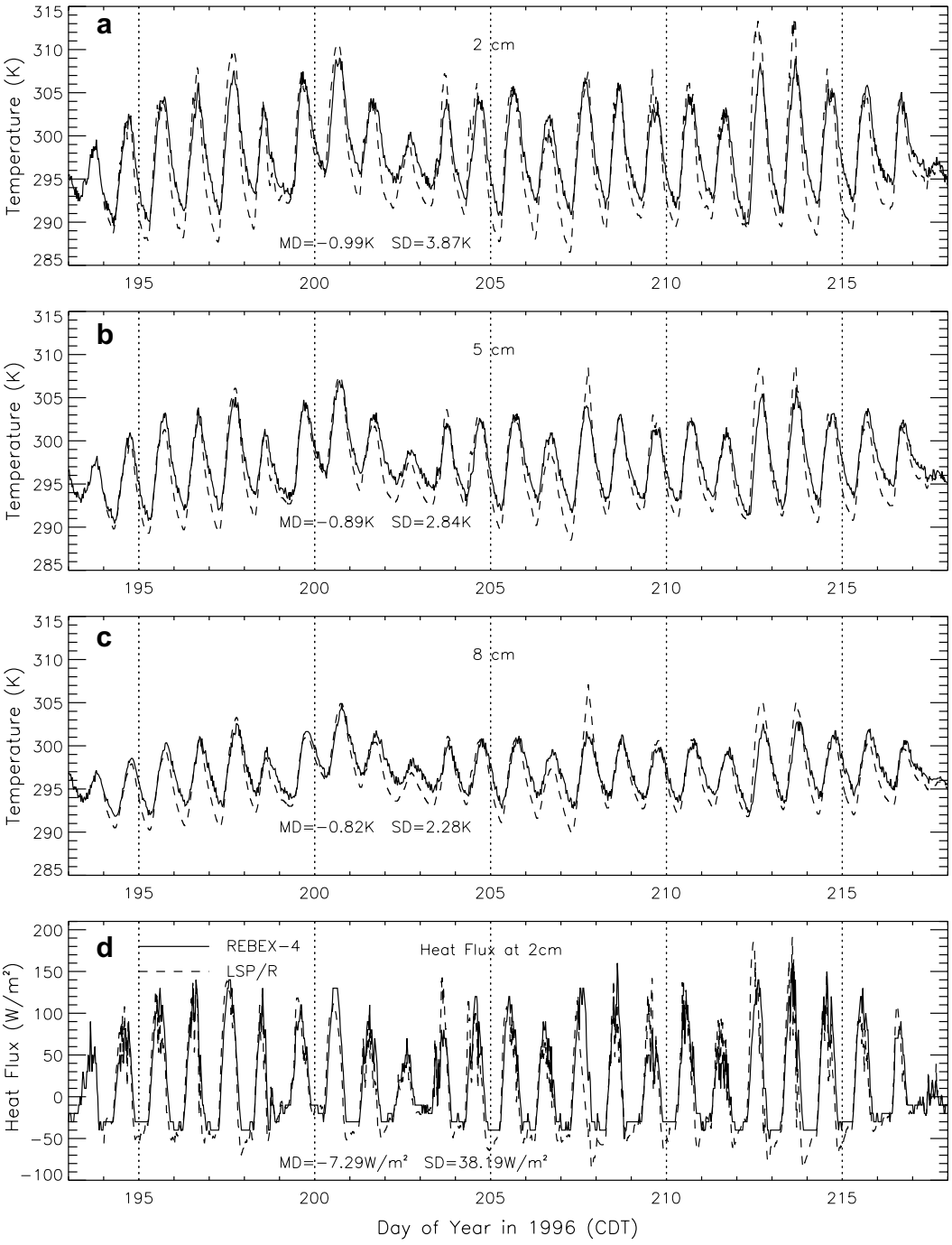

Fig. 4. A comparison of the estimated and the observed soil temperatures for the bare soil at (a) 2 cm (b) 5 cm (c) 8 cm, and (d) heat fluxes at 2 cm. MD is the mean difference, estimated − observed, and SD is the standard deviation.

depths of 2, 5, and 8 cm, and soil heat fluxes at 2 m, respectively. Overall, the model captures the phases of the diurnal variations in the soil temperatures. The modeled diurnal amplitudes at the depths of 2, 5, and 8 cm match well with the observations, as indicated by low mean differences between the estimated and the observed temperatures and their standard deviations. The amplitudes of the modeled temperatures at 2 cm are slightly higher than observed but the amplitudes at 5 and 8 cm match the observed values well. Modeled heat fluxes at 2 cm matched well with the observed fluxes as shown in Fig. 4d. This implies that the modeled energy transport below the depth of 2 cm is realistic, whereas the transport in the upper 2 cm is overestimated. Slight underestimates in the nighttime heat fluxes by the LSP/R model are similar to those found in other modeling studies [70]. The mean differences between the model and the observed temperatures are as much as twice the instrument error of ±0.5 K. Similar differences were found by Mohr et al. [48], Chen [7] and Whitfield et al. [70] in their model calibration and intercomparison studies.

Fig. 5a–c compares the estimated and the observed soil moisture at depths of 2, 5, and 8 cm, respectively. There were two significant rain events during REBEX-4, on DOY 198 (10.8 mm) and DOY 217 (8.3 mm). Several minor rain events of ⩽2 mm occured on DOY 193, 196, 203, 208, 209, 210, 211, 212, and 216. The model estimates realistic mean moisture values at the observed depths as given in. However, the estimated and the observed moisture at 2 cm are approximately 180° out of phase. The observed values shown in the Fig. 5a have not been corrected for temperature and their phases track the thermal variations in the soil. The period of the TDR probe-signal is sensitive to the changes in soil temperature [24] and result in these phase differences and also the stronger diurnal variations for observed moisture values than the model estimates at 8 cm. The values for mean differences in volumetric soil moisture between the LSP/R model and the

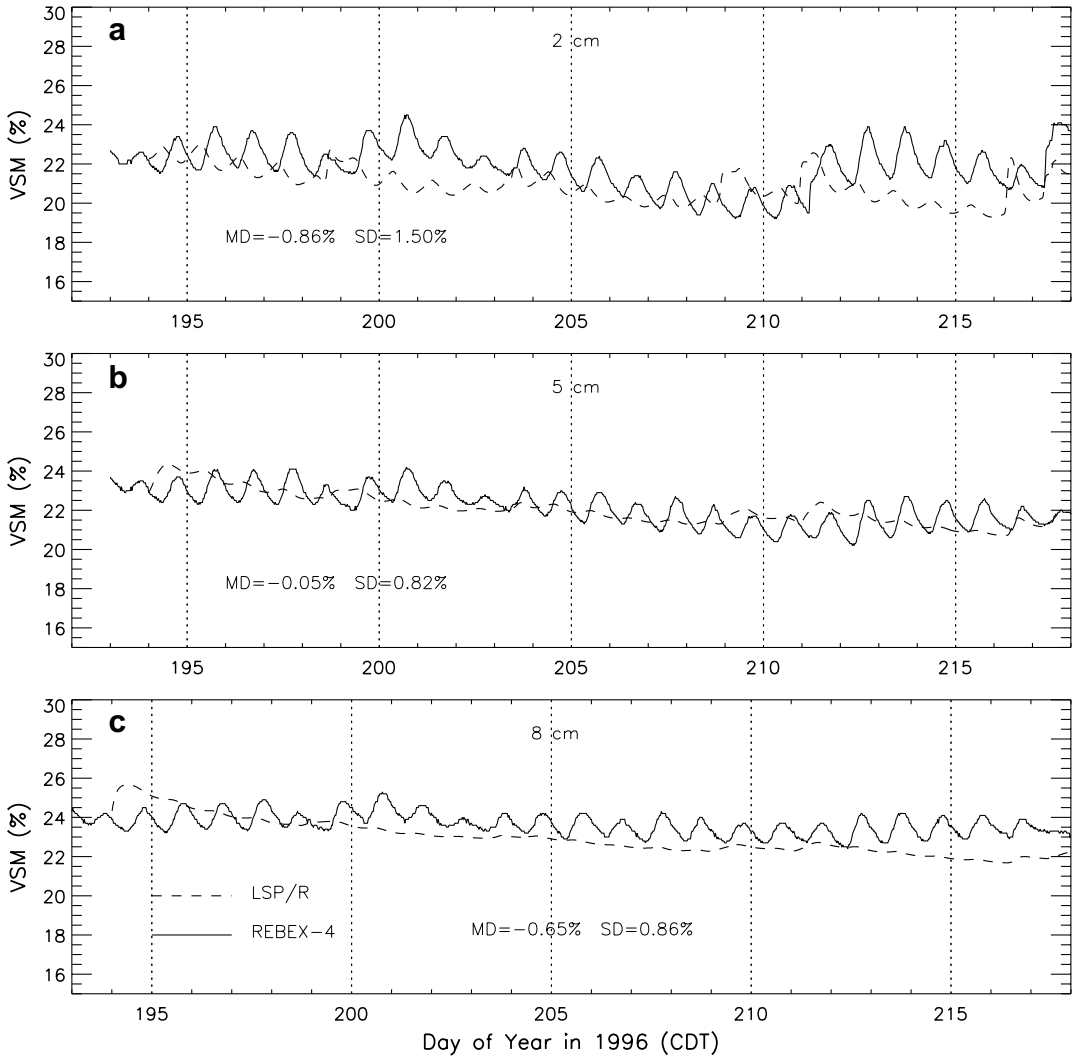

Fig. 5. A comparison of the estimated and the observed soil moisture at (a) 2 cm (b) 5 cm and (c) 8 cm. MD is the mean difference, estimated − observed, and SD is the standard deviation.

observations are similar to those from other studies. For example, Shao and Henderson-Sellers [61] and Mohr et al. [48] obtained differences of ±3% and ±5%, respectively during the PILPS phase 2(b) comparisons. Whitfield et al. [70] found differences of about ±3% between the LSP component of the LSP/R model and the observed soil moisture values for a prarie wetland.

Fig. 6 shows the estimated and the observed horizontally polarized (H-pol) soil brightness at 19 GHz. the Only the results at H-pol are presented here because H-pol brightness is more sensitive to soil moisture and surface features, such as roughness at our observation angles during REBEX-4 [64]. The phases of the diurnal variations are captured well, but mean values in the model are underestimated by ~70 K. Even though the artificially created bare soil site was somewhat smoothed by disking, the surface could not be modeled as a smooth surface at 19 GHz. Schmugge et al. [58] found similar large differences (~30 K) between the airborne observations at 1.4 GHz and the calculated brightness using the smooth-surface approximation. They attributed the differences to surface roughness. Later, Choudhury et al. [8] demonstrated that roughness effects could account for such large differences (as great as 50 K at 1.4 GHz) with their simplistic semi-empirical reflectivity model. As the roughness effects increase with frequency, larger differences could be expected at 19 GHz. Because surface roughness measurements were not conducted during the REBEX-4 experiment. We used a reflectivity model developed by Wang et al. [69] to investigate the effect of roughness on brightness estimates during REBEX-4. In the model, the Fresnel reflectivity is modified using two empirical parameters, roughness height h, and polarization mixing ratio Q. The reflectivity at polarization p is,

$$r_p(\theta) = [Qr_{0q}(\theta) + (1-Q)r_{0p}(\theta)]\exp(-hG(\theta)) \quad (6)$$

where r_{0p} and r_{0q} are the smooth surface reflectivities at polarizations p and q, and at incidence angle θ, and $G = 1$. Although, both h and Q increase with frequency, the dependence of Q is stronger, while that of h is not. The values for h and Q varied between 0–0.6 and 0–0.3, respectively [69]. For 19 GHz, $h = 0.8$ and $Q = 0.2$ produced the best fit between the observed and the estimated soil brightness at H-pol during REBEX-4 (Fig. 6). The value of h required to provide the best fit lay outside the range of values that Wang et al. [69] used. Theoretically, as the roughness of a surface increases compared to wavelength, the surface emissivity approaches that of a blackbody, i.e, the brightness temperature approaches its physical temperature. Consequently, the H-pol brightness increased significantly when a rough surface model was used.

4.6.2. Brome grass

The LSP/R model simulated the land surface processes for 22 days from DoY 196 (July 14) through 218 (August 5) in 1996. The Figs. 7 and 8 compare the observed and the modeled temperatures of canopy, thatch, and soil at the depths of 2, 4, 8, 32, and 64 cm and provide the mean differences and their standard deviations between the estimated and the observed temperatures and heat fluxes. The model canopy and thatch temperatures match well with the observed temperatures, as seen by their low differences. The model temperatures of the deeper layers of 32 and 64 cm match well with those observed during REBEX-4. However, the model estimates in the top 16 cm have a lower mean by ~5 K and are phase-shifted with respect to the observed temperatures. This indicates an incorrect heat conductive flux below 2 cm. The soil physical properties obtained from the soil survey might not represent the soil conditions at the undisturbed grass-site due to presence of organic matter. We included organic matter only in the upper 5 cm of the soil. The underestimated temperatures and amplitudes could also be an indication of unrealistic initial moisture profiles used in the grass model. As mentioned earlier, the profiles were obtained from a diurnal experiment conducted three days before the start of the simulation. The model estimates of soil moisture could not be evaluated during the calibration due to sensor problems. Moisture storage in the thatch could also be significant at this site and affect the water budget [5].

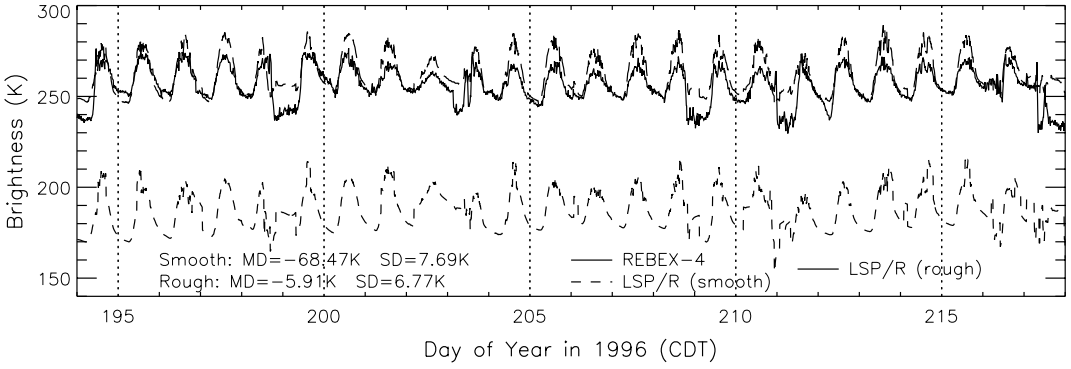

Fig. 6. A comparison of the estimated and the observed H-pol brightness at 19 GHz for bare soil using the smooth surface approximation and the rough surface model by Wang et al. [69]. MD is the mean difference, estimated − observed, and SD is the standard deviation.

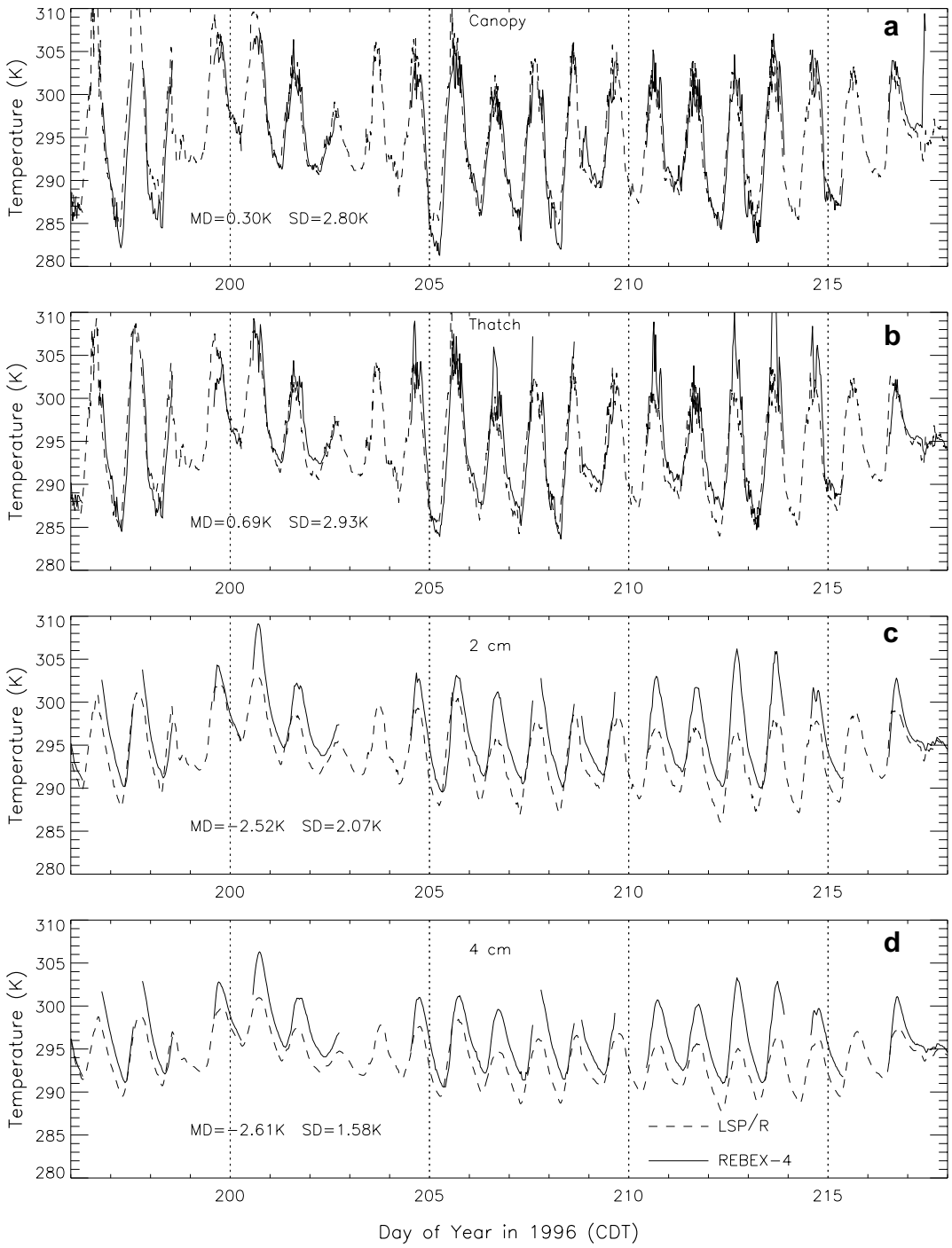

Fig. 7. A comparison of the estimated and the observed temperatures at the grass site. (a) Canopy; (b) thatch, and soil at (c) 2 cm (d) 4 cm. MD is the mean difference, estimated − observed, and SD is the standard deviation.

Heat fluxes into the ground at 2 cm match well the observed values (Fig. 9), which implies that the energy exchanges between thatch, canopy, and soil are being realistically modeled, and that the correct amount of thermal energy is being transported into the soil. As in the bare soil model, underestimates in nighttime fluxes are similar to those found in other modeling studies, for example [70].

Fig. 10 shows the model estimated and observed H-pol terrain brightness at 19 GHz. Estimated brightness matches observed brightness well. Approximately, 98% of the total emission at 19 GHz is from the canopy during the REBEX-4, when the values for canopy biomass were up to 3 kg/m^2 and the smooth surface approximation for the soil in the model did not result in big differences as those observed for the bare soil site. This could also be

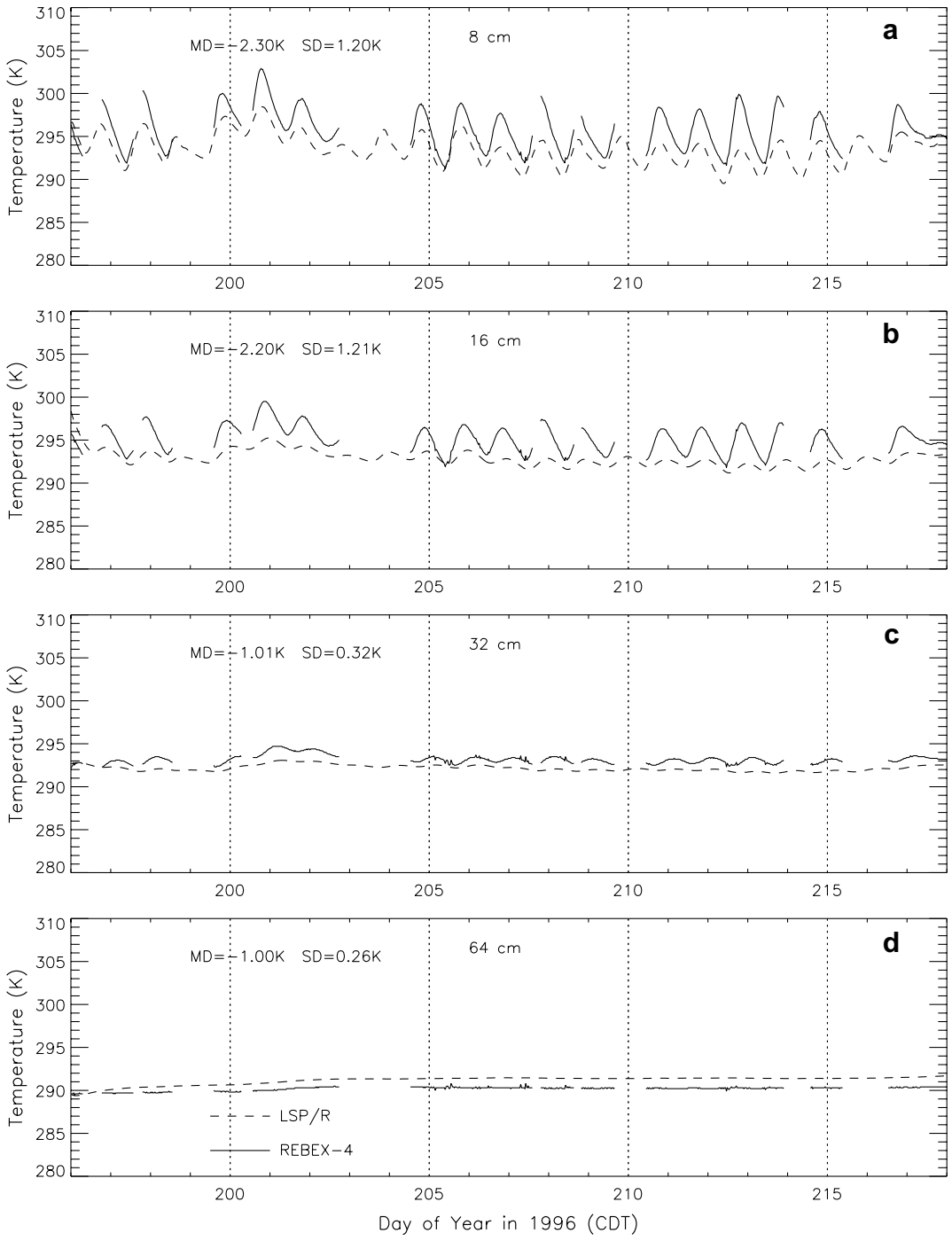

Fig. 8. A comparison of the estimated and the observed soil temperatures at the grass site. (a) 8 cm (b) 16 cm (c) 32 cm and (d) 64 cm. MD is the mean difference, estimated − observed, and SD is the standard deviation.

due to soil surface being smoother under the thatch layer for vegetation-covered soils.

Accurate H-pol brightness predictions reflect accurate canopy moisture and temperature estimates by the model, and validate use of the simple canopy emission model of a homogeneous cloud over a smooth surface. Low brightness temperatures are observed on rainy days, DoY 208, 209, 211, and 212 (Fig. 10).

5. Conclusions

The LSP/R model was calibrated for bare soil and brome grass using the data from the REBEX-4 experiment. It provided realistic estimates of soil moisture and temperature profiles to be used with a microwave for assimilating brightness observations, rather than assimilating soil moisture retrieved semi-emipirically from brightness observa-

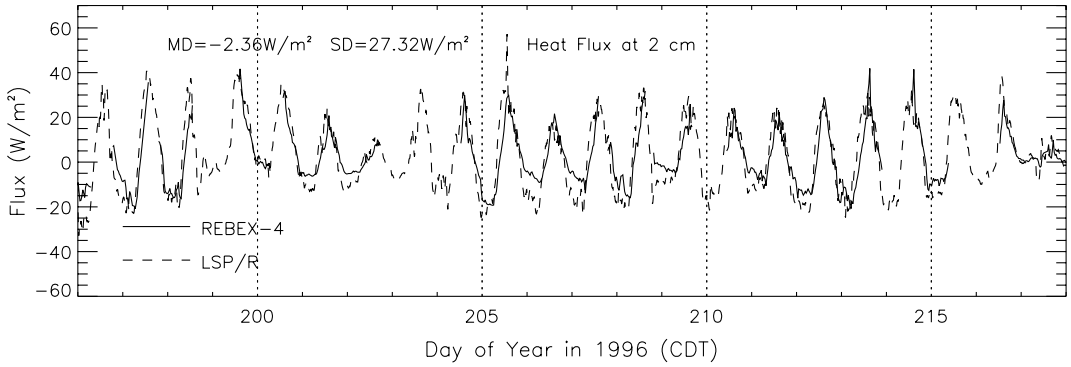

Fig. 9. A comparison of the estimated and the observed heat fluxes into the ground at 2 cm for the grass site. MD is the mean difference, estimated − observed, and SD is the standard deviation.

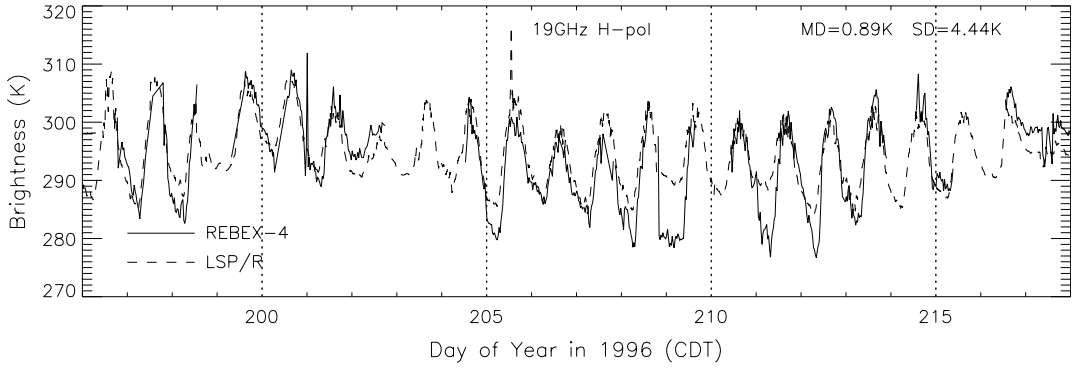

Fig. 10. A comparison of the estimated and the observed terrain brightness at 19 GHz for the grass site. MD is the mean difference, estimated − observed, and SD is the standard deviation.

tions. Because the LSP model is a physically based diagnostic model of moisture and energy transport in soil, it offers insights about linkage between control and movement of soil moisture and microwave signature. Future research using such LSP models should examine estimates of unconstrained parameters more closely to minimize the need of site-specific calibration for the intended application.

In the microwave emission model, the dielectric sensitivity to soil moisture was significantly masked by surface roughness at 19 GHz, introducing a need to use empirical roughness parameter values unless roughness is known. Soil roughness was not a significant issue for grass-covered soils because most of the brightness contribution at 19 GHz is from grass and the soil may be smoother under the thatch in these conditions. Integrated LSP/R models, such as the one in this study, can also be used to understand sensitivity of microwave signatures to changes in weather forcings and soil conditions for different terrain types.

Acknowledgements

This research was supported by grants from the NASA Land Surface Hydrology program and from the Alfred Sloan Foundation. We thank the anonymous reviewers for providing comments and suggestions to improve the manuscript. We also acknowledge the staff at the USGS EROS Data Center, Sioux Falls, SD for their hospitality and technical support during REBEX-4. Special thanks are due to Dr. David Meyer who willingly acted as a contact person to monitor the field set-up in SD. We worked closely with Drs. Linda Abriola (Tufts University) and Avery Demond (University of Michigan) to model soil properties and transport processes. We thank them for their helpful advice and input.

References

[1] Arya S. Introduction to meteorology. New York: Academic Press Inc.; 1988.
[2] Beljaars A, Viterbo P, Miller M, Betts A. The anomalous rainfall over the US during July 1993 – sensitivity to land–surface parametrization and soil moisture. Month Weather Rev 1996;124(3):362–83.
[3] N. Bliss, Personal communication; 1997.
[4] Bonan G. A land surface model (LSM Version 1.0) for ecological, hydrological, and atmospheric studies: technical description and user's guide. Tech. Rep. NCAR/TN-417+STR, Climate and Global Dynamics Division, NCAR.
[5] Brye K, Norman J, Bundy L, Gower S. Water-budget evaluation of prairie and maize ecosystems. Soil Sci Soc Am J 2000;64:715–24.
[6] Camillo P, Gurney R, Schmugge T. A soil and atmosphere boundary layer model for evapotranspiration and soil moisture studies. Water Res 1983;19(2):371–80.

[7] Chen T. Cabauw experimental results from the project of intercomparison of land–surface parameterization schemes. J Clim 1997;10:1194–215.
[8] Choudhury B, Schmugge T, Newton R, Chang A. Effect of surface roughness on the microwave emission from soils. J Geophys Res 1979;84:5699–706.
[9] Chung Y. A snow-soil-vegetation-atmosphere transfer/radiobrightness model for wet snow. Ph.D. thesis, University of Michigan; 2007.
[10] Crow W, Wood E. The assimilation of remotely sensed soil brightness temperature imagery into a land-surface model using ensemble kalman filtering: a case study based on ESTAR measurements during SGP97. Adv Water Resour 2003;26:137–49.
[11] de Vries D. Simultaneous transfer of heat and moisture in porous media. Trans Am Geophys Union 1958;39(5):909–16.
[12] de Vries D. Thermal properties of soils. Physics of plant environment. New York: Interscience Publishers; 1963. p. 210–35.
[13] Dickinson R, Henderson-Sellers A, Kennedy P. Biosphere–atmosphere transfer scheme (BATS) version 1e as coupled the NCAR Community Climate Model. Tech. Rep. NCAR/TN-387+STR, Climate and Global Dynamics Division, NCAR; 1993.
[14] Dickinson R, Henderson-Sellers A, Kennedy P, Wilson M. Biosphere–atmosphere transfer scheme (BATS) for the NCAR Community Climate Model. Tech. Rep. NCAR/TN-275+STP. Atmospheric Analysis and Prediction Division, NCAR; 1986.
[15] Dobson M, Ulaby F, Hallikainen M, El-Rayes M. Microwave dielectric behavior of wet soil – part II: dielectric mixing models. IEEE Trans Geosci Remote Sensing 1985;GE-23:35–46.
[16] England A, Galantowicz J. Moisture in a grass canopy from SSM/I radiobrightness. In: Proceedings of second tropical symposium on combined optical – microwave earth and atmospheric sensing; 1995. p. 12–4.
[17] Entekhabi D, Nakamura H, Njoku E. Solving the inverse problem for soil moisture and temperature profiles by sequential assimilation of multifrequency remotely sensed observations. IEEE Trans Geosci Remote Sensing 1994;32(2):438–48.
[18] Galantowicz J. Microwave radiometry of snow-covered grasslands for the estimation of land–atmosphere energy and moisture fluxes. Ph.D. thesis, University of Michigan; 1995.
[19] Galantowicz J, England A. Field data report for the first Radiobrightness Energy Balance Experiment (REBEX-1): October 1992–April 1993. Tech. Rep. Rad. Lab. Tech. Note RL-904, University of Michigan, Ann Arbor, MI; 1993.
[20] Galantowicz J, England A. Seasonal snowpack radiobrightness interpretation using a SVAT-linked emission model. J Geophys Res 1997;102(D18):21933–46.
[21] Galantowicz J, Entekhabi D, Njoku E. Tests of sequential data assimilation for retrieving profile soil moisture and temperature from observed l band radiobrightness. IEEE Trans Geosci Remote Sensing 1999;37(4):1860–70.
[22] Goodison B, Metcalfe J, McNichol D, Davey M, Le H. Participation in REBEX-4: data collection and completion phase report. Technical Report, Atmospheric Environment Service, Canada; 1996.
[23] Goodison B, Metcalfe J, McNichol D, Davey M, Le H. Participation in REBEX-4: Installation phase report. Technical Report, Atmospheric Environment Service, Canada; 1996.
[24] Hornbuckle B, England A. Radiometric sensitivity to soil moisture at 1.4 GHz through a corn crop at maximum biomass. Water Res 40 (W10204), doi:10.1029/2003WR002931; 2004.
[25] Houser P, Shuttleworth W, Famiglietti J, Gupta H, Syed K, Goodrich D, et al. Integration of soil moisture remote sensing and hydrologic modeling using data assimilation. Water Res 1998;34(12):3405–20.
[26] Jackson R, Reginato RJ, Kimball BA, Nakayama FS. Diurnal soil-water evaporation: comparison of measured and calculated soil-water fluxes. Soil Sci Soc Am Proc 1974;38:861–6.
[27] Jackson T, O'Neill P. Temporal observations of surface soil moisture using a passive microwave sensor. Remote Sens Env 1987;21:281–96.
[28] Jackson T, Schmugge T, O'Neill P. Passive microwave remote sensing of soil moisture from an aircraft platform. Remote Sens Env 1984;14:135–42.
[29] Judge J. Land surface process and radiobrightness modeling of the great plains. Ph.D. thesis. University of Michigan; 1999.
[30] Judge J, Abriola L, England A. Numerical validation of the land surface process component of an LSP/R model. Adv Water Resour 2003;26:733–46.
[31] Judge J, England A. Field data report for the fourth radiobrightness energy balance experiment (REBEX-4): June–September 1996. Tech. Rep. Rad. Lab. Tech. Note RL-974, University of Michigan; 1999.
[32] Judge J, England A, Hornbuckle BDL, Boprie C, Kim E. Field data report for the fifth radiobrightness energy balance experiment (REBEX-5). Tech. Rep. Rad. Lab. Tech. Note RL-964, University of Michigan; 1998.
[33] Judge J, England A, Crosson CLW, Hornbuckle B, Boprie D, Kim E, et al. A growing season land surface process/radiobrightness model for wheat-stubble in the southern great plains. IEEE Trans Geosci Remote Sensing 1999;37(5):2152–8.
[34] Judge J, Galantowicz J, England A. Freeze/thaw classification for prairie soils using SSM/I radiobrightnesses. IEEE Trans Geosci Remote Sensing 1997;35:827–32.
[35] Kerr Y, Waldteufel P, Wigneron JP, Marinuzzi JM, Font J, Berger M. Soil moisture retrieval from space: the soil moisture and ocean salinity (smos) mission. IEEE Trans Geosci Remote Sensing 2001;39(8):1729–35.
[36] Kim E. Remote sensing of land surface conditions in arctic tundra regions for climatological applications using microwave radiometry. Ph.D. thesis, University of Michigan; 1999.
[37] Kim E, England A. Field data report for radiobrightness energy balance experiment 3 (REBEX-3), 9/94-9/95, Alaskan north slope. Tech. Rep. Rad. Lab. Tech. Note RL-918, University of Michigan; 1998.
[38] Kimball B, Jackson R, Reginato R, Nakayama F, Idso S. Comparison of field-measured and calculated soil-heat fluxes. Soil Sci Soc Am J 1976;40:18–25.
[39] Lai S, Tiedje J, Erickson A. In situ measurement of gas diffusion coefficients in soils. Soil Sci Soc Am Proc 1976;40:3–6.
[40] Lakshmi V. A simple surface temperature assimilation scheme for use in land surface models. Water Res 2000;36(12):3687–700.
[41] Liang X, Lettenmaier D, Wood E, Burges S. A simple hydrologically based model of land surface water and energy fluxes for general circulation models. J Geophys Res 1994;99(D7):14415–28.
[42] Liang X, Lettenmaier D, Wood E, Burges S. One-dimensional statistical dynamical representation subgrid spatial variability of precipitation in the 2-layer variable infiltration capacity model. J Geophys Res 1996;101(D16):21403–22.
[43] Lin X, Smerdon JE, Pollack AE, H. A model study of the effects of climate precipitation changes on ground temperatures. J Geophys Res 108 (D7), Art. No. 4230; 2003.
[44] Liou Y, England A. Annual temperature and radiobrightness signatures for bare soils. IEEE Trans Geosci Remote Sensing 1996;34(4):981–90.
[45] Liou Y, England A. A land surface process/ radiobrightness model with coupled heat and moisture transport in soil. IEEE Trans Geosci Remote Sensing 1998;36(1):273–86.
[46] Liou Y, England A. A land surface process/radiobrightness model with coupled heat and moisture transport for freezing soils. IEEE Trans Geosci Remote Sensing 1998;36(2):669–77.
[47] Liou Y, Galantowicz J, England A. A land surface process/radiobrightness model with coupled heat and moisture transport for prairie grassland. IEEE Trans Geosci Remote Sensing 1999;37(4):1848–59.
[48] Mohr K, Famiglietti J, Boone A, Starks P. Modeling soil moisture and surface flux variability with an untuned land surface scheme: a case study from the southern great plains 1997 hydrology experiment. J Hydrometeor 2006;1:154–69.
[49] Mualem Y. A new model for predicting the hydraulic conductivity of unsaturated porous media. Water Res Res 1976;12(3):513–22.

[50] Nestrud L, Bourne W, Wennblom J, Wiesner W. Soil Survey of Minnehaha County, South Dakota. United States Department of Agriculture, Soil Conservation Service; 1964.
[51] Noilhan J, Planton S. A simple parametrization of land surface processes for meterological models. Month Weat Rev 1989;536–549(March).
[52] Peixoto J, Oort A. Physics of climate. New York: American Institute of Physics; 1992.
[53] Philip J, de Vries D. Moisture movement in porous materials under temperature gradients. Trans Am Geophys Union 1957;38(2):222–32.
[54] Reichle RH, DE, McLaughlin D. Downscaling of radiobrightness measurements for soil moisture estimation: a four-dimensional variational data assimilation approach. Water Res. Res 2001;37(9):2353–2364 (September).
[55] Reichle R, McLaughlin D, Entekhabi D. Variational data assimilation of microwave radiobrightness observations for land surface hydrologic applications. IEEE Trans Geosci Remote Sensing 2001;39(8):1708–18.
[56] Rossi C, Nimmo J. Modeling of soil water retention from saturation to oven dryness. Water Res Res 1994;30(3):701–8.
[57] T Schmugge, T Jackson. A dielectric model of the vegetation effects on the microwave emission from soils. IEEE Trans Geosci Remote Sensing 1992;30(4):757–60.
[58] Schmugge T, Wilheit T, Webster W, Gloersen P. Remote sensing of soil moisture with microwave radiometers II. Tech. Rep. TN D-8321, NASA; 1976.
[59] Sellers P, Mintz Y, Sud Y, Dalcher A. A Simple Biosphere model SiB for use within general circulation models. J Atmos Sc 1986;43(6):505–31.
[60] Sellers WD. Physical climatology. Chicago: The University of Chicago Press; 1965.
[61] Shao Y, Henderson-Sellers A. Validation of soil moisture simulation in land surface parameterization schemes with hapex data. Global Planet. Change 1996;13:11–46.
[62] Trenberth KE. Climate system modeling. New York: Cambridge University Press; 1995.
[63] Ulaby F, El-Rayes M. Microwave dielectric spectrum of vegetation-PartII: dual-dispersion model. IEEE Trans Geosci Remote Sensing 1987;GE-25(September):550–7.
[64] Ulaby F, Moore R, Fung A. Microwave remote sensing active and passive, vol. I. Massachussetts: Artech House; 1981.
[65] Ulaby F, Moore R, Fung A. Microwave remote sensing active and passive, vol. III. Ma ssachussetts: Artech House; 1986.
[66] Ulaby F, Razani M, Dobson M. Effects of vegetation cover on the microwave radiometeric sensitivity to soil moisture. IEEE Trans Geosci Remote Sensing 1983;GE-21:51–61.
[67] Verseghy S, McFarlane N, Lazare M. CLASS-A Canadian land suface scheme for GCMs.ii. vegetation model and coupled runs. Int J Climatology 1993;13:347–70.
[68] Walker J, Houser P. A methodology for initializing soil moisture in a global climate model: assimilation of near-surface soil moisture observations. J Geophys Res 2001;106(D11):11761–74.
[69] Wang J, O'Neill P, Jackson T, Engman E. Multifrequency measurements of the effects of soil moisture, soil texture, and surface roughness. IEEE Trans Geosci Remote Sensing 1983;GE-21(1):44–50.
[70] Whitfield B, Jacobs J, Judge J. Intercomparison study of land surface process model and the common model for a prairie wetland in florida. J Hydrometeor 2006;7(6):1247–58.